DOI: 10.1002/chem.201000627

Conversion of Methane to Methanol: Nickel, Palladium, and Platinum (d^9) Cations as Catalysts for the Oxidation of Methane by Ozone at Room Temperature

Andrea Božović,[a] Stefan Feil,[a] Gregory K. Koyanagi,[a] Albert A. Viggiano,[b] Xinhao Zhang,[c] Maria Schlangen,[c] Helmut Schwarz,*[c] and Diethard K. Bohme*[a]

Dedicated to Reinhart Ahlrichs on the occasion of his 70th birthday

Abstract: The room-temperature chemical kinetics has been measured for the catalytic activity of Group 10 atomic cations in the oxidation of methane to methanol by ozone. Ni^+ is observed to be the most efficient catalyst. The complete catalytic cycle with Ni^+ is interpreted with a computed potential energy landscape and, in principle, has an infinite turnover number for the oxidation of methane, without poisoning side reactions. The somewhat lower catalytic activity of Pd^+ is reported for the first time and also explored with DFT calculations. Pt^+ is seen to be ineffective as a catalyst because of the observed failure of PtO^+ to convert methane to methanol.

Keywords: C–H activation · density functional calculations · methanol · oxidation · ozone · transition metals

Introduction

The economically important conversion of methane to methanol continues to provide a chemical challenge and constitutes a "holy grail".[1] The C–H bond strength of methane is substantial at 102.7 ± 2.0 kcal mol^{-1}, while the thermodynamic affinity of methane for atomic oxygen, *OA*, to form methanol is moderately high at 90.7 kcal mol^{-1}.[2] This makes the direct gas-phase oxidation of methane by strong oxidants such as O_3 ($OA(O_2) = 25.5$ kcal mol^{-1})[2] and N_2O ($OA(N_2) = 40.0$ kcal mol^{-1})[2] very exothermic at room temperature, but the oxidation is impeded by activation energy barriers associated with C–H bond activation.[3] This has spawned a search for effective catalysts. Atomic metal and metal cluster ions have received particular attention because they provide an extra electrostatic energy of interaction that can reduce activation barriers and so lead to substantial enhancements in reaction rates.[4] Here we demonstrate that atomic metal cations can catalyze the oxidation of methane by transporting an O atom from ozone to the methane molecule as illustrated in Scheme 1.

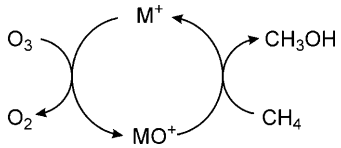

Scheme 1. Catalytic cycle for the homogeneous oxidation of methane with ozone, mediated by atomic metal cations.

The thermodynamic window[5] for catalysis by O-atom transport from ozone to methane with atomic metal cations requires that $25.5 < OA(M^+) < 90.7$ kcal mol^{-1}. Since the upper boundary condition for $OA(M^+)$ favors late over

[a] Dr. A. Božović, Dr. S. Feil, G. K. Koyanagi, Prof. Dr. D. K. Bohme
Department of Chemistry, York University
Toronto, ON, M3J 1P3 (Canada)
Fax: (+1) 416-736-5936
E-mail: dkbohme@yorku.ca

[b] Dr. A. A. Viggiano
Air Force Research Laboratory, Space Vehicles Directorate
29 Randolph Rd., Hanscom Air Force Base, MA 01731-3010 (USA)

[c] Dr. X. Zhang, Dr. M. Schlangen, Prof. Dr. H. Schwarz
Institut für Chemie, Technische Universität Berlin
Strasse des 17. Juni 135, 10623 Berlin (Germany)
Fax: (+49) 30-314-21102
E-mail: Helmut.Schwarz@mail.chem.tu-berlin.de

Supporting information for this article is available on the WWW under http://dx.doi.org/10.1002/chem.201000627.

early transition metal cations, we have chosen to investigate the catalytic activity of d^9 (Group 10) cations Ni^+ ($OA = 63.2 \pm 1.2$ kcal mol^{-1}),[6] Pd^+ ($OA = 33.6 \pm 2.5$ kcal mol^{-1}),[7] and Pt^+ ($OA = 75.1 \pm 1.6$ kcal mol^{-1}).[8]

Previous measurements have provided some insight into the kinetics of the second leg of the cycle shown in Scheme 1 with NiO^+ and PtO^+ (but apparently not with PdO^+). NiO^+ has been observed to produce $Ni^+ + CH_3OH$ exclusively with an efficiency of 20%,[9] whereas $Pt^+ + CH_3OH$ production was reported to proceed with PtO^+ on 25% of the reactive collisions along with a major (75%) production of $PtCH_2^+ + H_2O$ with a total reaction rate coefficient of 1.05×10^{-9} cm^3 molecule^{-1} s^{-1}.[10] We have investigated these two methane reactions, as well as that with PdO^+, in a flow tube experiment and also report here the first measurements of the kinetics of the first leg of the catalytic cycles. Furthermore, we have computed the potential energy surfaces (PES) for the $M^+/O_3/CH_4$ couples (M = Ni, Pd) using DFT to assess the experimental results.

Results and Discussion

The reactions of the bare metal cations with ozone all were observed to be fast, $k \geq 4.0 \times 10^{-10}$ cm^3 molecule^{-1} s^{-1}, and "clean", they produced only the metal oxide cation (see Table 1). Since $IE(O_3)$ is quite high (12.53 ± 0.08 eV),[2] electron transfer to these metal cations is endothermic by at least 3.57 eV. The reaction kinetics for the three metal oxide cations with methane were found to be much more diverse. Ion profiles recorded with methane addition are shown in Figure 1. Up to five different channels, those given in reaction (1), were observed in the proportions indicated.

Table 1. Rate coefficients and efficiencies for reactions of d^9 atomic-metal cations M^+ with O_3 and of their metal monoxide cations MO^+ with CH_4 at room temperature using ESI/qQ/SIFT/QqQ mass spectrometry. Also included are the overall efficiencies Φ_{cycle} for the catalytic reduction of O_3 by CH_4.

M^+	k[a]/Φ[b] (Φ_{ox})[b]	MO^+	k[a]/Φ[b] (Φ_{red})[b]	Products	Φ_{cycle}[c]
Ni^+	4.0/0.41 (*0.41*)	NiO^+	1.7/0.16 (*0.16*)	Ni^+	*0.066*
Pd^+	4.8/ 0.55 (*0.55*)	PdO^+	0.083/ 0.0083 (*0.0065*)	Pd^+ (78%) $PdOCH_2^+$ (15%) $PdO^+(CH_4)$ (7%)	*0.0036*
Pt^+	7.8/0.96 (*0.96*)	PtO^+	10/1.0	$PtCH_2^+$ (98%) PtH_2^+ (2%)	–

[a] k is the total reaction rate coefficient measured in units of 10^{-10} cm^3 molecule^{-1} s^{-1} with an uncertainty estimated to be ±30%. [b] The efficiency, Φ, is defined as k/k_c, where k_c is the collision rate coefficient, calculated by using the algorithm of the modified variational transition state/classical trajectory theory developed by Su and Chesnavich.[13] Subscripts "*ox*" and "*red*" indicate the oxidation of the bare metal ion and the reduction of the metal oxide ion, respectively, by O-atom transfer. [c] Φ_{cycle} is defined as $\Phi_{ox} \times \Phi_{red}$.[5]

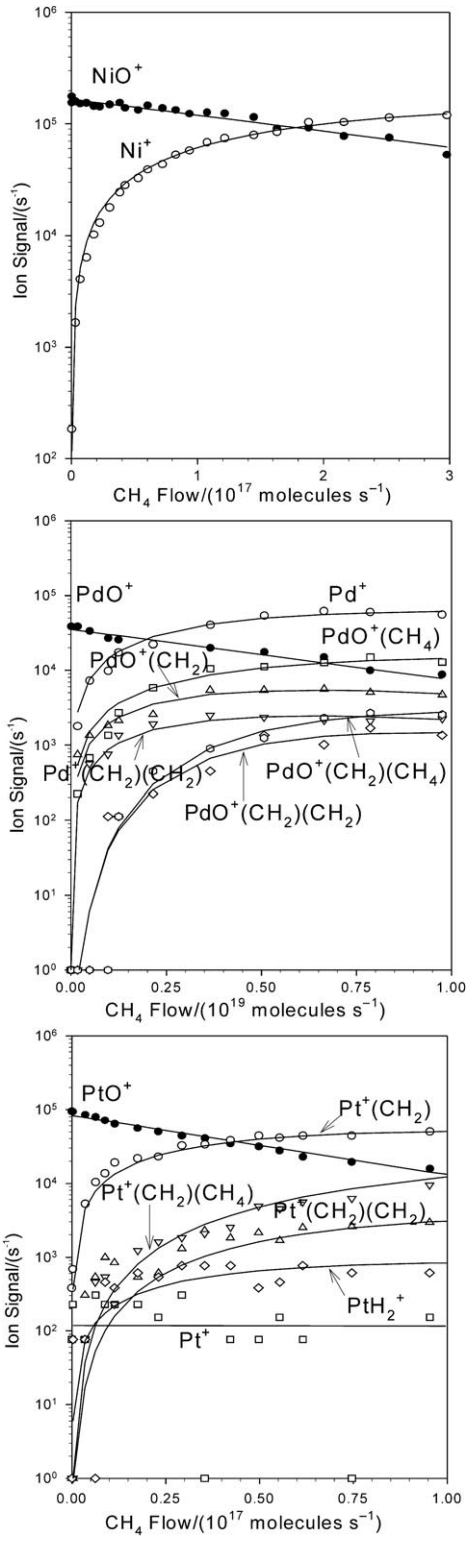

Figure 1. Reaction profiles measured for the reactions of NiO^+, PdO^+, and PtO^+ with CH_4 in helium buffer gas at 295 ± 3 K and 0.35 ± 0.01 Torr.

$$MO^+ + CH_4 \rightarrow M^+ + CH_3OH \quad (1a)\mathrm{M} = \mathrm{Ni}(100\%), \mathrm{Pd}(78\%)$$

$\rightarrow MCH_2^+ + H_2O$ (1b)M = Pt(98%)

$\rightarrow MOCH_2^+ + H_2$ (1c)M = Pd(15%)

$\rightarrow MO^+(CH_4)$ (1d)M = Pd(7%)

$\rightarrow MH_2^+ + CH_2O$ (1e)M = Pt(2%)

Channel (1a), the second leg of the catalytic cycle under investigation, is exothermic by −27.5, −57.1, and −15.6 kcal mol^{-1} for the reactions of NiO^+, PdO^+, and PtO^+, respectively.[2,6–8] Only NiO^+ exhibited pure formation of the atomic cation along with methanol, as indicated previously;[9] we are able to report that it reacts fast with a 41% efficiency (see Table 1). PdO^+ also produced mainly the atomic cation (78%) with minor channels of H_2 elimination (15%) and methane addition (7%). The platinum oxide cation was observed to react with methane at the collision limit, predominantly to dehydrate the intermediate (98%) and *not to generate bare Pt*$^+$. Formation of PtH_2^+ and CH_2O was also observed but this channel is almost negligible, at 2%. The $PtCH_2^+$ reacts further with CH_4 to eliminate hydrogen and to add methane.[11] The very small signal at *m/z* of Pt^+ (0.1%) initially present in the spectrum does not increase with the addition of CH_4 into the reaction region (see Figure 1).[12]

Our result for the products of the PtO^+ reaction with methane differs from the previous FT-ICR observations by the Berlin group that reported $PtCH_2^+$ as a major product ion, 75%, and bare Pt^+ as a minor product ion, 25%.[10] However, much better agreement is found with the more recent results of new experiments in which PtO^+ was produced by pulsing N_2O into mass-selected $^{195}Pt^+$ ions that were generated by laser desorption/ionization from the solid metal. After additional mass selection and subsequent thermalization with pulsed Ar buffer gas, reactions of PtO^+ with leaked-in CH_4 were studied at a pressure of 8×10^{-9} mbar and short reaction times of 0.5 to 2 s. The branching ratios for the product ions $PtCH_2^+$, Pt^+, and PtH_2^+ were determined to be 94, 3, and 3%, respectively.

The gas-phase kinetics measured with our selected-ion flow tube tandem mass spectrometer at room temperature for the catalytic cycles leading to methanol formation from ozone and methane are summarized in Table 1. The experimental results indicate an interesting unambiguous trend in catalytic efficiency going down the periodic table with the d^9 transition-metal cations. Ni^+ appears to be best suited as a catalyst with no ozone side reactions, Pt^+ is not suitable as it is not regenerated in the reaction of its oxide cation with methane, and Pd^+ is intermediate in its performance as a catalyst.

A computed potential energy landscape for the catalysis mediated by M^+ (M = Ni and Pd) is given in Figure 2. The profile for the uncatalyzed oxidation of methane, overall very exothermic (−70.8 and −65.2 kcal mol^{-1} according to

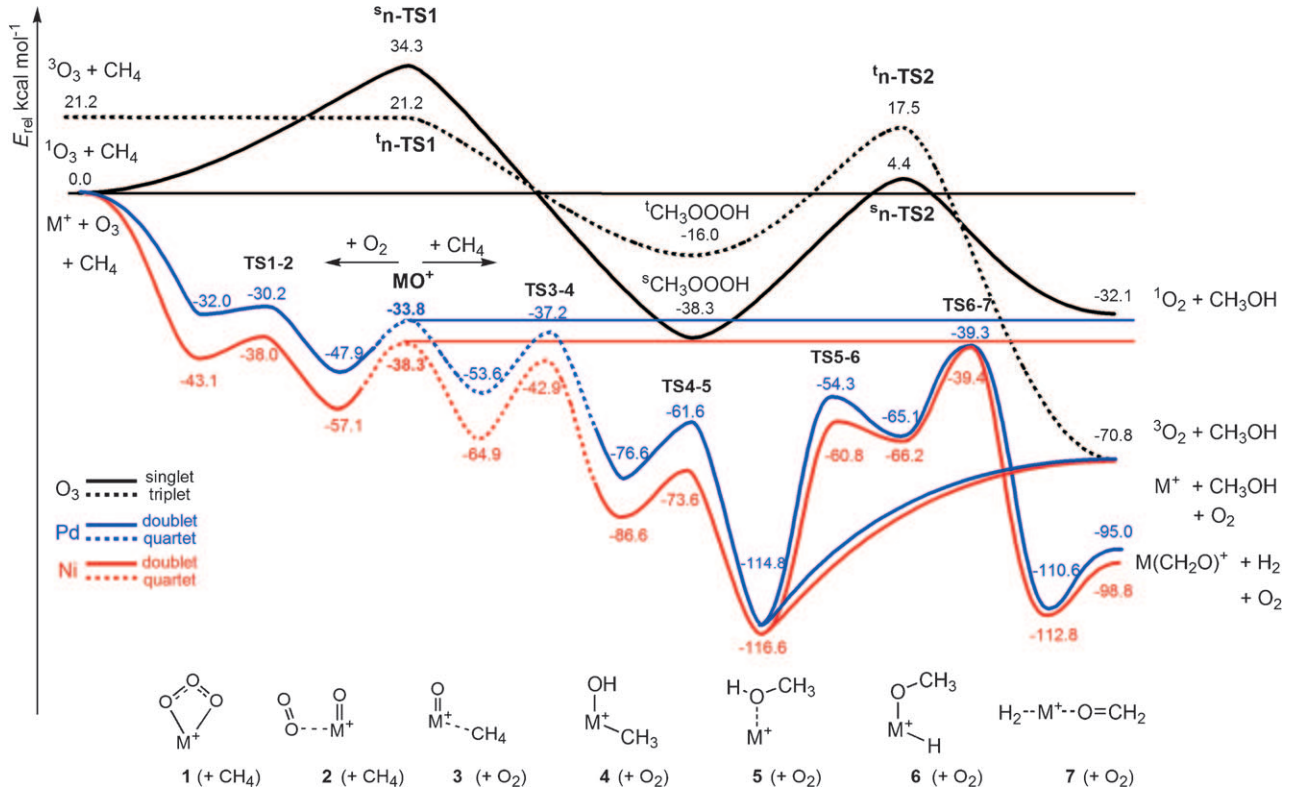

Figure 2. Potential-energy surfaces computed for the oxidation of CH_4 with O_3 in the absence (black lines) and presence of Ni^+ (red line) or Pd^+ (blue line) calculated at B3LYP/def2-TZVP. The dashed lines represent the pathways for the species in their higher electronic states. For clarity, only the electronic states in the lowest energy are shown for metal-mediated reactions.

the calculations and to published enthalpies of formation,[2] respectively), indicates a two-step reaction. Similar to silanes and germanes,[14] methane only forms a van der Waals complex with O_3 without stabilization. The structure ^{s}**n-TS1** corresponds to the concerted insertion of O_3 into a C–H bond of methane with a barrier of 34.3 kcal mol^{-1}. The hydrotrioxide intermediate $^{s}CH_3OOOH$ decomposes into methanol and singlet O_2, via a 1,3 H-shift transition state ^{s}**n-TS2**. Given the fact that singlet $^1O_2$ is generated by the ozonation of triethylsilane via triethylsilyl hydrotrioxide,[15] the spin inversion is not believed to occur along the reaction path, even though the high-spin H-abstraction transition state ^{t}**n-TS1** and the triplet product ($^3O_2$ + CH_3OH) are lower in energy. So the uncatalyzed oxidation of methane by ozone to form methanol is kinetically forbidden due to the overall barrier of 34.3 kcal mol^{-1} on the singlet state surface and the expected rather inefficient spin-orbit coupling.[16]

Since methane activation by PtO^+ has been extensively investigated both experimentally and computationally,[10,17] we focus here on Ni and Pd. The relevant computed M^+-catalyzed pathways are presented in Figure 2. In contrast to the uncatalyzed reaction, spin inversion can take place due to the efficient spin-orbit coupling of the metal-mediated reaction.[18] For the sake of clarity, the ionic pathways (in blue and red) are described as continuous surfaces consisting of two spin states and only the electronic states in the lowest energy are shown (see the Supporting Information for more details of other reaction pathways). The activation barrier for the O-atom insertion into methane is drastically lowered by the addition of a singly charged bare Ni^+ or Pd^+ cation.

The first step involves an O-atom transfer from ozone to M^+ on a doublet surface with the formation of MO^+ in their lowest (quartet) states and O_2 (triplet) with relative energies of −38.3 and −33.8 kcal mol^{-1} for Ni^+ and Pd^+, respectively. The transfers proceed smoothly since the transition states **TS1–2** are only a few kcal mol^{-1} higher in energy than the energies of the initial adducts **1**.

The next elementary reaction starts with an entrance channel of MO^+ ($^4\Sigma$) + CH_4. The similarity in the shapes of the PES of NiO^+ and PdO^+ also has been reported for methane activation by *neutral* NiO and PdO.[19] The channels toward $M(OH)^+$ + $^{\bullet}CH_3$[20] or $M(OCH_2)^+$ + H_2[10] are found to be thermodynamically less favorable than the observed products (see the Supporting Information). The CH_4/CH_3OH conversion by MO^+ proceeds through two steps, MO^+ insertion into a C–H bond and reductive elimination from $HOMCH_3^+$ (**4**) to generate **5**. The former step is rate-determining for the overall pathway. The small energy differences between **TS3–4** and the entrance channel, that is, 4.6 kcal mol^{-1} for NiO^+ and 3.4 kcal mol^{-1} for PdO^+, indicate a significant competition between the formation of **4** and the dissociation back to the reactants. So dissociation back to reactants is predicted to be more pronounced for the reaction of PdO^+ and this is qualitatively consistent with the experiments which recorded an efficiency for the PdO^+ reaction lower than that for NiO^+ (see Tables 1 and S1). The desired product, methanol, dissociates from the global minimum $M(CH_3OH)^+$ (**5**), regenerating bare M^+ and thus closing the catalytic cycle. One of the challenges of selective methane/methanol conversion is to prevent a further oxidation of methanol into formaldehyde.[21] As shown in Figure 2, the methanol complex **5** may undergo oxidative addition of the O–H bond to the metal center (**5** → **6**) followed by a dehydrogenation to yield $(H_2)M(OCH_2)^+$ (**7**). H_2 is then easily evaporated from **7**, giving the thermodynamically more favorable product $M(OCH_2)^+$. The barrier from **5** to $M(OCH_2)^+$ is determined by **TS6–7**, which lies closely below the entrance channel of MO^+/CH_4, amounts to 5.5 kcal mol^{-1} for Pd and 1.1 kcal mol^{-1} for Ni. Thus oxidation of **5** to generate $Pd(OCH_2)^+$ takes place slowly for PdO^+/CH_4, whereas it hardly occurs for NiO^+/CH_4, in line with the experimental observation that NiO^+/CH_4 gives Ni^+ + CH_3OH exclusively, whereas PdO^+/CH_4 affords $Pd(OCH_2)^+$ as side product.

Our computations are in good qualitative agreement with previous studies for the NiO^+/CH_4 toward methanol by Shiota and Yoshizawa.[18a] Additional reaction pathways were extensively investigated and these were compared with the $Pd^+/O_3/CH_4$ system. which has not been studied previously.[22] Our results explain the selective oxidation of methane to methanol by NiO^+; formation of the side products $NiOH^+$ + $^{\bullet}CH_3$ or $Ni(CH_2)^+$ + H_2O are thermodynamically unfavorable, and the side product $Ni(OCH_2)^+$ + H_2 is not kinetically accessible. In comparison, slight difference on the PES gives different reaction pattern for $Pd^+/O_3/CH_4$. While there exist some parallels for the "Group 10" metal hydride chemistry in their reactions with CH_4, there are subtle as well as fundamental differences, and as stated in a different context,[23] "the same and not the same" holds true once more.

Our computed $OA(Pd^+)$ of 47.8 kcal mol^{-1} is higher than the value of 33.6 ± 2.5 kcal mol^{-1} determined experimentally from the kinetic energy onset of PdO^+ by reaction of Pd^+ with O_2 and in agreement with the, albeit highly uncertain, value of 48 ± 23 kcal mol^{-1} determined from available thermochemical data.[7] The experimental value derived from the reaction of Pd^+ with O_2 might be underestimated due to the neglect of a possible impulsive pairwise mechanism.[7] Furthermore, a higher value also is expected for the O-atom affinity of Pd^+ from a comparison with the experimental values for the S-atom affinities of Ni^+ (56.7 kcal mol^{-1})[24] and Pd^+ (54.4 kcal mol^{-1}).[25]

The experiments show that the reaction of PtO^+ with CH_4 prefers another pathway which leads to the formation of $Pt(CH_2)^+$ + H_2O. Computations for this reaction have been reported by Schwarz and co-workers.[18] We have included a comparison of the PES reported for this reaction with those computed here for the reactions of NiO^+ and PdO^+ in the Supporting Information (Figure S2). In comparing the rate-determining steps, namely the first C–H bond activation to give $M(OH)(CH_3)^+$, we note that the relative energies of the rate-determining transition states are −5.9, −4.6, and −3.4 kcal mol^{-1} for PtO^+, NiO^+, and PdO^+, respectively. This is in line with the experimentally observed

order in overall reaction efficiency: PtO^+ (1.0) > NiO^+ (0.16) > PdO^+ (0.0083).

Conclusion

The room-temperature chemical kinetics has been measured for the catalytic activity of d^9 atomic cations in the oxidation of methane to methanol by ozone. Ni^+ is observed to be the most efficient catalyst and exhibits, in principle, an infinite turnover number for the oxidation of methane, without poisoning side reactions. The complete catalytic cycle with Ni^+ is interpreted with a computed potential energy landscape. A somewhat lower catalytic activity is observed for Pd^+ and reported for the first time. The DFT calculations account for this reduced efficiency in terms of a higher-energy rate-determining transition state. Pt^+ is seen to be ineffective as a catalyst because of the observed failure of PtO^+ to convert methane to methanol.

Both our experimental results and the interpretive potential energy landscapes in Figure 2 clearly point toward the efficient catalytic action of gaseous Ni^+ and Pd^+ ions in the conversion of methane to methanol in the presence of ozone in the gas phase. The challenge now becomes the generation of such gaseous (or surface?) ions in devices that provide practical applications.

Experimental Section

Experiments at York University were performed with a multi-source, multi-sector selected-ion flow tube tandem mass spectrometer, symbolized as ESI(ICP)/qQ/SIFT/QqQ.[26] The atomic cations Ni^+, Pd^+, and Pt^+ were generated from solutions of their salts by using an electrospray ionization (ESI) source with a microspray emitter needle. Nickel nitrate (Aldrich, p. a. $\geq$ 99.999%) and platinum chloride (Aldrich, p. a. $\geq$ 99.99%) were dissolved in a mix of HPLC grade methanol (Aldrich) and Millipore (18.2 mΩ) water (20:80 v/v). Acetonitrile (Aldrich, p. a. $\geq$ 99.8%) was used as a pure solvent in the ESI experiments of palladium acetate. The salt solutions were introduced directly into the electrospray source at a flow rate of 7 μL min^{-1}. A declustering potential of 200 V was applied to obtain sufficient amounts of bare metal ions. Metal oxide cations were formed in the orifice-skimmer region of the atmosphere-vacuum interface prior to the mass selection quadrupole by doping the interface gas, normally pure nitrogen, with 50 mL min^{-1} of 4% ozone in O_2. Ozone was generated in a O3V–0, OREC Inc. model laboratory ozone generator.[27] Oxygen from Liquid Carbonic was used directly.

The bare atomic or atomic oxide cations were mass selected and injected through a Venturi type aspirator into the flow tube that is flushed with helium at 0.35 ± 0.01 Torr. Before reaching the reaction region, the ions undergo multiple collisions with helium (ca. 4×10^5) to ensure thermalization. The large number of collisions with the helium buffer gas atoms should be sufficient to ensure that the atomic ions reach a translational temperature equal to the tube temperature of 292 ± 2 K prior to entering the reaction region. The bare atomic cations were allowed to react with ozone (4% ozone in oxygen), in a manner described in detail previously,[28] whereas the atomic oxide cations were allowed to react with methane (Matheson, C.P. Grade (99.97%)) added into the reaction region and then sampled along with product ions and analyzed in a triple quadrupole mass spectrometer. The contribution of reactions of the atomic ions with oxygen to those with ozone was negligible (<1%); we have previously studied the oxygen reactions separately.[29] Reactant and product ion signals were monitored as a function of the flow of the reagent gas. Primary rate coefficients were determined from the observed semi-logarithmic decay of the primary reactant ion intensity using pseudo first order kinetics an accuracy estimated to be ±30%.

The new Berlin measurements were performed by means of a Spectrospin CMS 47X FT-ICR mass spectrometer[30] equipped with a Smalley-type[31] cluster-ion source developed by Bondybey, Niedner-Schatteburg and co-workers.[32,33] In brief, the fundamental of a pulsed Nd:YAG laser ($\lambda = 1064$ nm, Spectron Systems) is focused onto a rotating platinum target to generate a metal plasma from which ion formation occurs by synchronization of a He pulse and subsequent supersonic expansion. After passing a skimmer, the ionic components of a molecular beam are transferred into the analyzer cell where they are trapped in the field of a 7.05 T superconducting magnet. PtO^+ was produced by pulsing-in N_2O into $^{195}Pt^+$ ions that were mass selected by means of the FERETS ion-ejection technique.[34]

Computational Section

The calculations were performed using the Gaussian03 package.[35] Geometries were optimized at the unrestricted UB3LYP level of theory[36] with the def2-TZVP basis set.[37] Frequency calculations were carried out for all optimized structures with the same method to verify the nature of the stationary points on the potential-energy surfaces (PESs) and to obtain the zero-point energy corrections. The connections between transition states and corresponding minima were verified using the intrinsic reaction coordinate technique (IRC).[38] Finally, all relative energies (corrected for ZPE contributions) are reported in kcal mol^{-1}.

Acknowledgements

D.K.B. acknowledges continued financial support from the National Research Council (Canada), the Natural Science and Engineering Research Council (Canada) and MDS SCIEX. As holder of a Canada Research Chair in Physical Chemistry, D.K.B. also thanks the contributions of the Canada Research Chair Program to this research. The research in Berlin was supported by the Fonds der Chemischen Industrie and the Deutsche Forschungsgemeinschaft "Cluster of Excellence: Unifying Conception in Catalysis". X.Z. acknowledges financial support from the Alexander von Humboldt-Stiftung.

[1] See, for example: a) W. Buijs, *Top. Catal.* **2003**, *24*, 73; b) G. A. Olah, A. Goeppert, G. K. S. Prakash, *Beyond Oil and Gas: The Methanol Economy*, Wiley-VCH, Weinheim, **2009**; c) R. Palkovits, C. v. Malotki, M. Baumgarten, K. Müllen, C. Baltes, M. Antonietti, P. Kuhn, J. Weber, A. Thomas, F. Schüth, *ChemSusChem* **2010**, *3*, 277.

[2] NIST-JANAF Themochemical Tables, NIST Chemistry Web Book; NIST Standard Reference Database, http://webbook.nist.gov/chemistry/.

[3] See, for example: F. J. Dillemuth, D. R. Skidmore, C. C. Schubert, *J. Phys. Chem.* **1960**, *64*, 1496.

[4] a) D. K. Böhme, H. Schwarz, *Angew. Chem.* **2005**, *117*, 2388; *Angew. Chem. Int. Ed.* **2005**, *44*, 2336; b) R. A. J. O'Hair, G. N. Khairallah, *J. Cluster Sci.* **2004**, *15*, 331; c) G. E. Johnson, R. Mitric, V. Bonacic-Koutecky, A. W. Castleman, Jr., *Chem. Phys. Lett.* **2009**, *475*, 1; d) D. Schröder, H. Schwarz, *Proc. Natl. Acad. Sci. USA* **2008**, *105*, 18114; e) G. E. Johnson, E. C. Tyo, A. W. Castleman, Jr., *Proc. Natl. Acad. Sci. USA* **2008**, *105*, 18108.

[5] V. Blagojevic, G. Orlova, D. K. Bohme, *J. Am. Chem. Soc.* **2005**, *127*, 3545.

[6] *Organometallic Ion Chemistry* (Ed.: B. S. Freiser), Kluwer, Dordrecht, **1996**.

[7] Y.-M. Chen, P. B. Armentrout, *J. Chem. Phys.* **1995**, *103*, 618.
[8] X-G. Zhang, P. B. Armentrout, *J. Phys. Chem. A* **2003**, *107*, 8904.
[9] M. F. Ryan, H. Schwarz, unpublished results, cited by D. Schröder, H. Schwarz, *Angew. Chem.* **1995**, *107*, 2126; *Angew. Chem. Int. Ed. Engl.* **1995**, *34*, 1973.
[10] R. Wesendrup, D. Schröder, H. Schwarz, *Angew. Chem.* **1994**, *106*, 1232; *Angew. Chem. Int. Ed. Engl.* **1994**, *33*, 1174.
[11] K. K. Irikura, J. L. Beauchamp, *J. Phys. Chem.* **1991**, *95*, 8344.
[12] We speculate that the very small initial signal at *m*/*z* 196 (Pt^+) may arise from incomplete separation of Pt^+ and PtO^+ in the mass selection prior to the flow tube or come from the reaction of PtO^+ with background impurities (e.g., CO).
[13] T. Su, W. J. Chesnavich, *J. Chem. Phys.* **1982**, *76*, 5183.
[14] J. Cerkovnik, T. Tuttle, E. Kraka, N. Lendero, B. Plesničar, D. Cremer, *J. Am. Chem. Soc.* **2006**, *128*, 4090.
[15] E. J. Corey, M. M. Mehrotra, A. U. Khan, *J. Am. Chem. Soc.* **1986**, *108*, 2472.
[16] a) J. N. Harvey, M. Aschi, *Phys. Chem. Chem. Phys.* **1999**, *1*, 5555; b) J. N. Harvey, S. Grimme, M. Woeller, S. D. Peyerimhoff, D. Danovich, S. Shaik, *Chem. Phys. Lett.* **2000**, *322*, 358; c) M. Tashiro, R. Schinke, *J. Chem. Phys.* **2003**, *119*, 10186; d) A. M. Mebel, M. Hayashi, V. V. Kislov, S. H. Lin, *J. Phys. Chem. A* **2004**, *108*, 7983; e) Y. Dede, X. Zhang, M. Schlangen, H. Schwarz, M.-H. Baik, *J. Am. Chem. Soc.* **2009**, *131*, 12634.
[17] M. Pavlov, M. R. A. Blomberg, P. E. M. Siegbahn, R. Wesendrup, C. Heinemann, H. Schwarz, *J. Phys. Chem.* **1997**, *101*, 1567.
[18] a) Y. Shiota, K. Yoshizawa, *J. Am. Chem. Soc.* **2000**, *122*, 12317; b) J. N. Harvey, *Phys. Chem. Chem. Phys.* **2007**, *9*, 331.
[19] D.-Y. Hwang, A. M. Mebel, *J. Phys. Chem. A* **2002**, *106*, 12072.
[20] a) D. Schröder, H. Schwarz, *Angew. Chem.* **1990**, *102*, 1468; *Angew. Chem. Int. Ed. Engl.* **1990**, *29*, 1433; b) A. Božović, D. K. Bohme, *Phys. Chem. Chem. Phys.* **2009**, *11*, 5940.
[21] For recent experimental and computational details on the selective C–H or O–H bond activation of CH_3OH, see: a) M. Schlangen, H. Schwarz, *Chem. Commum.* **2010**, *46*, 1878; b) M. Schlangen, H. Schwarz, *ChemCatChem.* **2010**, *2*, 799, and references therein.
[22] J. Roithová, D. Schröder, *Chem. Rev.* **2010**, *110*, 1170.
[23] M. Schlangen, H. Schwarz, *Angew. Chem.* **2007**, *119*, 5711; *Angew. Chem. Int. Ed.* **2007**, *46*, 5614.
[24] C. Rue, P. B. Armentrout, I. Kretzschmar, D. Schröder, H. Schwarz, *J. Phys. Chem. A* **2002**, *106*, 9788.
[25] P. B. Armentrout, I. Kretzschmar, *Inorg. Chem.* **2009**, *48*, 10371.
[26] G. K. Koyanagi, V. Baranov, S. Tanner, J. Anichina, M. J. Y. Jarvis, S. Feil, D. K. Bohme, *Int. J. Mass Spectrom.* **2007**, *265*, 295.
[27] See, for example: A. I. Fernandez, A. J. Midey, T. M. Miller, A. A. Viggiano, *J. Phys. Chem. A* **2004**, *108*, 9120.
[28] S. Feil, G. K. Koyanagi, A. A. Viggiano, D. K. Bohme, *J. Phys. Chem. A* **2007**, *111*, 13397.
[29] G. K. Koyanagi, D. Caraiman, V. Blagojevic, *J. Phys. Chem. A* **2002**, *106*, 4581.
[30] K. Eller, W. Zummack, H. Schwarz, *J. Am. Chem. Soc.* **1990**, *112*, 621.
[31] S. Maruyama, L. R. Anderson, R. E. Smalley, *Rev. Sci. Instrum.* **1990**, *61*, 3686.
[32] C. Berg, T. Schindler, M. Kantlehner, G. Niedner-Schatteburg, V. E. Bondybey, *Chem. Phys.* **2000**, *262*, 143.
[33] M. Engeser, T. Weiske, D. Schröder, H. Schwarz, *J. Phys. Chem. A* **2003**, *107*, 2855.
[34] R. A. Forbes, H. F. Laukien, J. Wronka, *Int. J. Mass Spectrom. Ion Processes* **1988**, *83*, 23.
[35] Gaussian 03, Revision E.01, M. J. Frisch, G. W. Trucks, H. B. Schlegel, G. E. Scuseria, M. A. Robb, J. R. Cheeseman, J. A. Montgomery, Jr., T. Vreven, K. N. Kudin, J. C. Burant, J. M. Millam, S. S. Iyengar, J. Tomasi, V. Barone, B. Mennucci, M. Cossi, G. Scalmani, N. Rega, G. A. Petersson, H. Nakatsuji, M. Hada, M. Ehara, K. Toyota, R. Fukuda, J. Hasegawa, M. Ishida, T. Nakajima, C. Adamo, J. Maramillo, R. Gomperts, R. E. Stratmann, O. Yazyev, A. J. Austin, R. Cammi, C. Pomelli, J. W. Ochterski, P. Y. Ayala, K. Morokuma, G. A. Voth, P. Salvador, J. J. Dannenberg, V. G. Zakrewski, S. Dapprich, A. D. Daniels, M. C. Strain, O. Farkas, D. K. Malick, A. D. Rabuck, K. Raghavachari, J. B. Foresman, J. V. Ortiz, Q. Cui, A. G. Baboul, S. Clifford, J. Cioslowski, B. B. Stefanov, G. Liu, A. Liashenko, P. Piskorz, I. Komaromi, R. L. Martin, D. J. Fox, T. Keith, M. A. Al-Laham, C. Y. Peng, A. Nanayakkara, M. Challacombe, P. M. W. Gill, B. Johnson, W. Chen, M. W. Wong, C. Gonzalez, J. A. Pole, Gaussian Inc., Wallingford CT, **2004**.
[36] a) A. D. Becke, *J. Chem. Phys.* **1993**, *98*, 5648; b) C. Lee, W. Yang, R. G. Parr, *Phys. Rev. B* **1988**, *37*, 785.
[37] a) F. Weigend, R. Ahlrichs, *Phys. Chem. Chem. Phys.* **2005**, *7*, 3297; b) Effective core potential (ECP) for Pd: B. Metz, H. Stoll, M. Dolg, *J. Chem. Phys.* **2000**, *113*, 2563; c) the basis sets were obtained from the Gaussian Basis Set Library EMSL at https://bse.pnl.gov/bse/portal; d) D. Feller, *J. Comput. Chem.* **1996**, *17*, 1571; e) K. L. Schuchardt, B. T. Didier, T. Elsethagen, L. Sun, V. Gurumoorthi, J. Chase, J. Li, T. L. Windus, *J. Chem. Inf. Model* **2007**, *47*, 1045.
[38] a) K. Fukui, *J. Phys. Chem.* **1976**, *80*, 4161; b) K. Fukui, *Acc. Chem. Res.* **1981**, *14*, 363; c) C. Gonzalez, H. B. Schlegel, *J. Chem. Phys.* **1989**, *90*, 2154; d) C. Gonzalez, H. B. Schlegel, *J. Phys. Chem.* **1990**, *94*, 5523.

Received: March 10, 2010
Published online: September 8, 2010

